8th World Congress on Structural and Multidisciplinary Optimization
June 1-5, 2009, Lisbon, Portugal

On the use of a truly–mixed formulation in topology optimization with global stress–constraints

Matteo Bruggi[1], Pierre Duysinx[2]

[1] Department of Structural Mechanics, University of Pavia, I27100 Pavia, Italy,
matteo.bruggi@unipv.it
[2] Department of Aerospace and Mechanical Engineering, University of Liège, 4000 Liège, Belgium,
p.duysinx@ulg.ac.be

1. Abstract
The work refers to the field of topology optimization for bidimensional structures and addresses the case in which global stress–constraints are considered to improve final designs.
Most of the previous research tackles this topic relying on classical displacement–based finite elements where stresses are recovered via post–processing techniques. The work conversely investigates the use of a truly–mixed formulation where stresses are independent variables of the problem while displacements play the secondary role of Lagrangian multiplier. The implemented discretization is based on a composite triangular element whose features may be advantageously exploited in stress–constrained topology optimization. The discretization is checkerboard–free and allows to tackle topology optimization with element–based constraints without introducing any additional filtering technique. The high accuracy in the evaluation of the average stresses is expected to improve the efficiency of the numerical procedure, especially in the case of a single global constraint that has to govern the whole domain. The adopted discretization also passes the robustness condition even in the case of incompressible materials and this allows to menage strength constraints also for rubber–like components.
Basing on these ideas, numerical investigations are carried out to test preliminary applications of the truly–mixed technique coupled with topology optimization and global stress–constraints. To handle the well–known singularity problem, that affects the constraints imposition, an alternative scheme is herein adopted instead of a classical ε–relaxation. An example where a homogenous stress distribution is expected is firstly tested, having the aim of pointing out the main features of the proposed procedure. Afterwards, numerical simulations address a classical L–shaped specimen, pointing out pros and cons of the approach.
2. Keywords: Topology optimization, global stress constraints, mixed finite elements, singularity problem.

3. Introduction
Stress constraints are of paramount importance in topology optimization, since the respect of the allowable strength of material is a fundamental requirement to achieve a feasible manufacturing. Despite this issue, most of the classical formulations based on the distribution of isotropic material addresses problems for topology optimization that assume the strain energy as objective function, thus taking care of the stiffness of the domain but neglecting its overall stress state [1]. To take into account this crucial aspect, alternative formulations have been developed in the last decades. They are mainly based on the minimization of the structural weight, subject to constraints on the stress threshold according to the strength of material. Two different schemes may be followed. The first one was originally introduced in [9] and consists in the adoption of a number of local constraints that control each element–wise stress value on the mesh that discretizes the domain. This approach allows for an affordable solution from the physical point of view, but pays a remarkable computational burden descending on the large number of constraints. Due to the need of reducing the computing efforts, an alternative procedure was presented in [10], adopting only one single global constraint instead of the large set implemented in the previous approach. An efficient choice for the evaluation of the overall stress state is represented by the so–called p–mean or p–norm constraints, as further detailed in the sequel. The adoption of one single measure of the stress field on the whole domain does not allow for a strict control of the peak values. However, this procedure considerably reduces the computational burden and is able to keep the average stress below a prescribed threshold.
According to the above discussion, a key point of stress–constrained topology optimization is the need

for an accurate numerical description of the stress field. Standard approaches resort to low order displacement–based schemes that recover element–wise stresses via post–processing techniques, i.e. additional numerical treatments on the derivatives of the primal variables. These procedures also affect the sensitivity computation within the optimization scheme and may cause a loss of accuracy of the whole procedure. The quality of the approximation of the stress field also descends from the order of the finite element shape functions. This means that low order displacement–based schemes, that are generally adopted not to increase the computational burden of the optimization, have the main counterpart of a poor resolution in stress evaluation. Moreover, they may exhibit numerical instabilities depending on the adopted density discretization, see i.e. the checkerboard phenomenon [1], or due to the compressibility of the considered material, see i.e. the locking phenomenon [8].
The present contribution has the aim of overcoming the above drawbacks by testing the adoption of a truly–mixed finite element scheme [5] within a topology optimization setting that implements global stress constraints [10]. The mixed formulation descends from the principle of Hellinger–Reissner and has stresses as main variables, while displacements play the role of Lagrangian multipliers. The adopted discretization is based on the composite element of Johnson and Mercier [11] that fully passes the stability condition, even in the case of incompressible material [3], and has been shown to be checkerboard–free [5]. This means that the proposed approach may also be used to tackle stress–constrained topology optimization of incompressible materials. Another appealing aspect of the adopted discretization resides in some peculiar features of its shape functions. Among the 15 dofs of the JM element, three unknowns accurately define the average value of the stress on the whole triangle. This allows for an efficient (and computationally cheap) handling of the global constraints originally discussed in [10]. The singularity problem is tackled by an alternative approach as introduced in [4], that is herein embedded in the p–norm and p–mean stress measures. The contribution addresses preliminary numerical investigations on two benchmark examples. The first refers to a rectangular domain where a simple two–bar design is expected to be achieved under pure shear actions. The second refers to an L–shaped cantilever, dealing with the reduction of the stress peak in its corner zone.

4. Truly–mixed formulation

A few fundamental theoretical remarks on the truly–mixed approach are herein recalled, as further discussed in [3] and implemented e.g. in [5]. Considering the continuum formulation, let $\Omega \in R^2$ be a regular domain bounded by $\partial\Omega$ and $\underline{\underline{\underline{\underline{C}}}}$ the elasticity tensor of the linear elastic isotropic material. Notations $\underline{\underline{\sigma}}$ and $\underline{u}$ denote the unknown stress and displacement fields, respectively, while $\underline{g}$ is the vector body load. $\underline{u}_d$ denotes the prescribed displacement on Γ_d, while $\underline{f}_t$ the prescribed traction on Γ_t, being, as usual, $\Gamma = \Gamma_d \cup \Gamma_t$. The truly–mixed variational principle is hold by two groups of equations. The first one couples constitutive law and compatibility, that are tested by a virtual stress field $\underline{\underline{\tau}}$. The second one reduces to equilibrium, that is conversely tested by means of a virtual displacement field, $\underline{v}$. One therefore ends up with the following "truly–mixed" weak formulation that reads: find $(\underline{\underline{\sigma}}, \underline{u}) \in H \times W$ such that $\underline{\underline{\sigma}} \cdot \underline{n} \,|_{\Gamma_t} = \underline{f}_t$ and

$$\begin{cases} \displaystyle\int_\Omega \underline{\underline{\underline{\underline{C}}}}^{-1} \underline{\underline{\sigma}} : \underline{\underline{\tau}} dx + \int_\Omega \underline{\mathrm{div}}\, \underline{\underline{\tau}} \cdot \underline{u} dx = \int_{\Gamma_d} \underline{u}_d \cdot (\underline{\underline{\tau}} \cdot \underline{n}) ds, \quad \forall \underline{\underline{\tau}} \in H, \\ \displaystyle\int_\Omega \underline{\mathrm{div}}\, \underline{\underline{\sigma}} \cdot \underline{v} dx = -\int_\Omega \underline{g} \cdot \underline{v} dx, \qquad\qquad \forall \underline{v} \in W. \end{cases} \tag{1}$$

where $\underline{n}$ denotes the normal vector to the boundary. Important features of the formulation reside in the choice of the functional spaces for displacements and stress, that may be respectively defined as:

$$W = \left[L^2(\Omega)\right]^2, \tag{2}$$

and

$$H = H(\underline{\mathrm{div}}\,;\Omega) = \left\{ \underline{\underline{\tau}} : \tau_{ij} = \tau_{ji},\ \tau_{ij} \in L^2(\Omega),\ \underline{\mathrm{div}}\, \underline{\underline{\tau}} \in W \right\}. \tag{3}$$

The above equations may be re–written according to the classical compact scheme for saddle point problems, that reads: find $(\underline{\underline{\sigma}}, \underline{u}) \in H \times W$ such that $\underline{\underline{\sigma}} \cdot \underline{n} \,|_{\Gamma_t} = \underline{f}_t$ and:

$$\begin{cases} a(\underline{\underline{\sigma}}, \underline{\underline{\tau}}) + b(\underline{\underline{\tau}}, \underline{u}) = f(\underline{u}_d, \underline{\underline{\tau}} \cdot \underline{n}), \qquad \forall \underline{\underline{\tau}} \in H(\Omega), \\ b(\underline{\underline{\sigma}}, \underline{v}) \qquad\qquad = g(\underline{g}, \underline{v}), \qquad\quad \forall \underline{v} \in W(\Omega). \end{cases} \tag{4}$$

Each scalar product $(\cdot,\cdot)$ in Eqn. (4) may be straightforwardly derived from a comparison with Eqn. (1). No further detail is discussed for brevity sake, while peculiar attention is devoted in the next paragraphs to the finite element discretization, that has a crucial role in the stress–constrained procedure herein implemented.

4.1. The JM composite element

The discretization of the above variational principle is accomplished through the composite element of Johnson and Mercier [11], that has the important feature of passing the inf–sup condition [3] in the discretized form, notwithstanding the bulk modulus of the analyzed material. This means that this finite element choice is fully stable even in the presence of incompressible materials and no fluctuation or locking trouble is expected in the achieved result (see e.g. [14] for a discussion on this topic referring to the adoption of the so–called u–p formulations.) Each JM element K is further subdivided into three

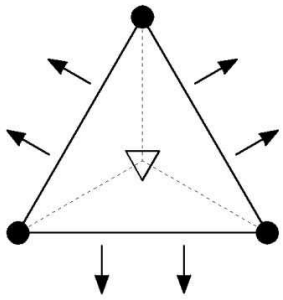

Figure 1: JM composite element - Stress–flux dofs (arrows), stress tensor dofs (central triangle) and displacement dofs (circles).

sub-triangles T_j. The displacement field is discretized via linear functions on the whole element, as done in classical displacement–based interpolation as the constant strain triangle (CST). Coming to the stress field, the interpolating components are linear within each sub–triangle and the continuity of the stress-flux between each sub-edge is a priori imposed. Denoting with $P_1(T_j)$ the space of the polynomials of degree ≤ 1 on T_j, it is worth recalling the space of approximation of stresses as:

$$H_h = \{\ \underline{\underline{\sigma}}_h \in H(\underline{\mathrm{div}}\ ;\Omega),\ \underline{\underline{\sigma}}_h \in H(\underline{\mathrm{div}}\ ;K),\ \underline{\underline{\sigma}}_h|_{T_j} \in [P_1(T_j)]_s^{2\times 2}\ ,\ j=1,2,3\}, \tag{5}$$

where $\underline{\underline{\sigma}}_h$ may be derived according to the 15 degrees of freedoms defined in [11], i.e.:

$$\int_{e_i} (\underline{\underline{\sigma}}_h \cdot \underline{n}) \cdot \underline{w} ds, \quad \forall \underline{w} \in (P_1(e_i))^2, \quad i=1,2,3, \tag{6}$$

$$\int_K \underline{\underline{\sigma}}_h : \underline{\underline{w}} dx, \quad \forall \underline{\underline{w}} \in (P_0(K))_s^{2\times 2}, \tag{7}$$

being e_i the i–th edge of the triangular element. Among the above 15 degrees of freedom, the three unknowns introduced in Eqn. (7) are defined as the average of the components of the stress tensor on the whole triangle. This provide an accurate measure of the overall element–wise stress state that may be therefore recovered via a few main unknowns of the elastic problem. At this stage it must be noticed that an affordable measure of the element–wise Von Mises stress σ_{VM} may be directly handled, in an averaged form, performing the following basic computation on each triangle:

$$\sigma_{VM} = \sqrt{\sigma_{xx}^2 + \sigma_{yy}^2 - \sigma_{xx}\sigma_{yy} + 3\sigma_{xy}^2}. \tag{8}$$

The stress σ_{VM} is in fact derived taking into account only σ_{xx}, σ_{yy} and σ_{xy}, that are the average values on the whole element of the components of the stress tensor $\underline{\underline{\sigma}}$ in a plane state, i.e. the three dofs defined in Eqn. (7). To assess the accuracy of the adopted procedure and the numerical advantages allowed by the adoption of Eqn. (7) in the evaluation of the element–wise σ_{VM}, let briefly consider the benchmark problem in Figure 2. The cantilever was analytically solved in [16] and is herein adopted to present a comparison on converge results in the evaluation of the stress field between the classical displacement–based constant stress triangle (CST) and the herein implemented JM element. The stress recovered from

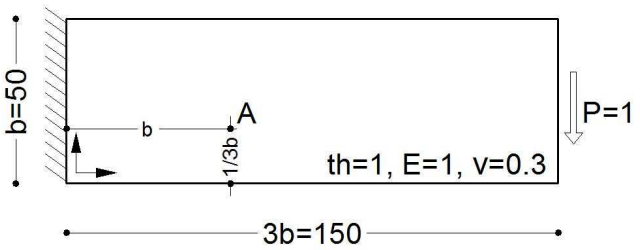

Figure 2: The cantilever problem of [16].

the three average dofs of Eqn. (7) are denoted as JM3, while the ones interpolated via the full set of dofs in both Eqn. (6) and Eqn. (7) are referred to as JM15. Figure 3 shows two sets of convergence curves that refer to the point A depicted in Figure 2. The plot on the left may be intended as a kind of *patch test* for the JM elements. Its linear stress shape functions immediately recover the first order σ_{xx} distribution on the specimen, while the constant approximation of CST needs more refinement to achieve the expected convergence. The plot on the right shows the approximation of a parabolic shear profile σ_{xy} in the two considered discretizations. The evaluation via JM15 achieves the expected fast convergence. It must be remarked however that the performances of JM3 are much higher than the displacement–based CST triangle. This preliminary discussion allows to conclude that the JM element provides an affordable evaluation of the stress field. Moreover, the adoption of element–wise stress measures based on the only three average dofs of Eqn. (7) allows to save computational time without losing too much in terms of accuracy. This is a crucial issue for the implementation of the topology optimization schemes presented in the sequel, since iterative procedures take a remarkable benefit of this choice when handling constraints and their sensitivities.

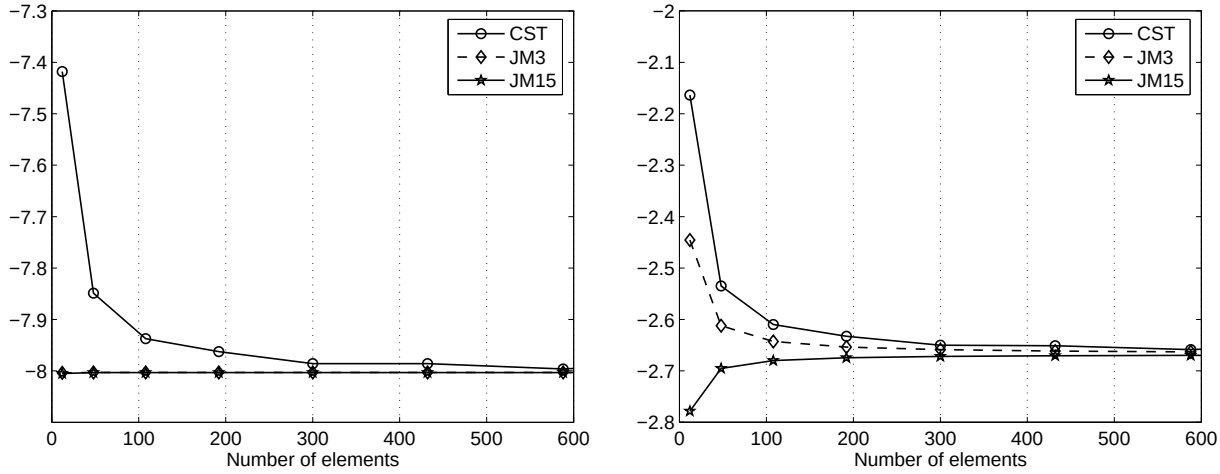

Figure 3: σ_{xx} (L) and σ_{xy} (R) for point A of the cantilever problem in Figure 2.

5. Stress–constrained topology optimization

The following section introduces the stress–constrained minimum weight formulation that implements the truly–mixed finite element scheme presented in the previous sections. It points out peculiar aspects of the proposed procedure that mainly resides in the adoption of an alternatively–relaxed global stress constraint and its numerical treatment within the truly–mixed scheme.

5.1. An alternative relaxation for the p–mean global constraint.

The contribution focuses on the adoption of a single global constraint instead of the implementation of a number of element–wise local enforcements, as originally introduced in [9]. The approach has the main benefit of remarkably reducing the computational effort requested to the minimization procedure, since optimizers usually exhibit numerical troubles for an increasing number of constraints. Reference is made to the work [7] for an original application of the technique and to [10] for a detailed discussion on the

properties of the p–norm and p–mean. It is worth recalling that both the norms may be intended as a global measure of the overall stress state, having peculiar differences in their asymptotic behavior. For a given value of the controlling parameter p, the maximum stress value is always bounded from above by the p–norm and from below by the p–mean. This means that the p–mean is expected to gain numerical tractability with respect to the p–norm, since it is easier for the minimizer to achieve feasible solutions with such a behavior of the constraint. The p–mean is therefore implemented in the present work, taking also into account the adoption of suitable schemes to avoid the arising of the so–called singularity problem, see e.g. [6]. The unrelaxed version of the global constraint p–mean reads:

$$\left[\frac{1}{N}\sum_{i=1}^{N}\left(\frac{\sigma_{VM,i}}{\rho_i^{\eta}\sigma_Y}\right)^p\right]^{1/p} \leq 1, \tag{9}$$

where $\sigma_{VM,i}$ and ρ_i are, respectively, the Von Mises stress and the density of the i–th element among the N ones that make the adopted mesh. σ_Y is the allowed strength of material and η is the exponent of the power law that interpolates the Young modulus of the material, according to the classical SIMP (see [1]). The main parameter p controls the constraint, meaning that a high value of p requires a more homogeneous stress peaks distribution. Such a numerical scheme is not able to completely remove low density regions within the considered stress–constrained minimum weight problems, due to the above mentioned singularity problem. Non–zero stresses may in fact arise at zero density, vanishing the reliability of the numerical procedure. To overcome this problem one may resort to a mathematical relaxation based on the ε–approach of [6]. According to [10], the following relaxed version of the p–mean constraint may be derived:

$$\left[\frac{1}{N}\sum_{i=1}^{N}\left(max\{0,\frac{\sigma_{VM,i}}{\rho_i^{\eta}\sigma_Y}+\varepsilon-\frac{\varepsilon}{\rho_i}\}\right)^p\right]^{1/p} \leq 1, \tag{10}$$

where the introduction of the additional max function is needed to avoid undesired negative contributions within the overall sum on N, due to peculiar properties of the ε–relaxation. The herein implemented scheme adopts another numerical treatment, as derived in [4]. The desired relaxation at low densities is achieved by replacing the exponent η of Eqn. (9) with an exponent q next to η, such that $q < \eta$. One therefore gets the following relaxed expression of the p–mean constraint, as it will be implemented in the sequel of the paper:

$$\left[\frac{1}{N}\sum_{i=1}^{N}\left(\frac{\sigma_{VM,i}}{\rho_i^{q}\sigma_Y}\right)^p\right]^{1/p} \leq 1. \tag{11}$$

As detailed in [4] this choice allows for the desired mathematical relaxation at low densities, without introducing any additional bias in the full material regions. The procedure may be used within the framework of a classical continuation approach, in an iterative scheme where $q \to \eta$. However, the absence of any bias at $\rho = 1$ allows for feasible results for any admissible choice of q producing pure 0–1 designs. It is worth remarking that Eqn. (11) simply consists in a variation of the original constraint of Eqn. (9). The achieved relaxation does not produce any negative contributions within the overall sum on N and therefore does not call for additional modifications of the original global constraint, as done in Eqn. (10).

5.2. Minimum weight formulation

All the numerical studies presented next may be framed within the following stress–constrained minimum weight setting:

$$\begin{cases} \min\limits_{0<\rho\leq 1} & \mathcal{W} \\ \\ \text{s.t.} & \begin{bmatrix} A_{\sigma\sigma}(\rho) & B_{\sigma u} \\ B_{u\sigma} & 0 \end{bmatrix} \begin{Bmatrix} \sigma \\ u \end{Bmatrix} = \begin{Bmatrix} f \\ g \end{Bmatrix} \\ \\ & \left[\frac{1}{N}\sum_{i=1}^{N}\left(\frac{\sigma_{VM,i}}{\rho_i^{q}\sigma_Y}\right)^p\right]^{1/p} \leq 1 \end{cases} \tag{12}$$

where $\mathcal{W}$ is the objective function, i.e. the weight of the structure. The first constraint of the minimization process is the solution of the elasticity problem, that is tackled in its truly–mixed form, as it may be straightforwardly derived from Eqn. (4). The second constraint is the relaxed p–mean in Eqn. (11),

i.e. the global enforcement on the stress peaks all over the domain. It must be remarked that the above procedure takes full advantage of the mixed nature of the variational principle. The stresses used in the computation of the global p–mean are in fact main variables of the elasticity problem. They are directly recovered from the solution of the saddle–point setting and do not call for any post–processing technique, as commonly done in displacement–based methods. To speed up the computations, the evaluation of σ_{VM} is carried out by means of Eqn. (8), that only resorts to the three average degrees of freedom in Eqn. (7), instead of the full set of the fifteen JM–element unknowns. The preliminary convergence study presented in the numerical section suggests that this choice preserves a high accuracy in the evaluation of the stress field, having the main benefit of a limited computational cost.

5.3. Computational details

We recall that the mixed matrix of Eqn. $(12)_2$ depends on the design variables ρ only through the complementary energy of the block $A_{\sigma\sigma}$, that embeds the constitutive law. Moreover the saddle–point nature of the problem calls for ad hoc sparse solvers that manage matrixes which are not positive definite [12, 13].

In the preliminary simulations presented in the sequel it has been chosen to adopt an element–wise discretization for the density unknowns, without the introduction of any filtering procedure. This allows to exploit the checkerboard–free nature of the JM–based finite element scheme, in order to investigate the behavior of the relaxed global constraint of Eqn. (11) without any additional bias.

Referring to the minimization setting, the Method of Moving Asymptotes (MMA) [15] has been adopted in the first set of simulations, in conjunction with the analytical computations of the gradients. A crucial issue of the proposed procedure mainly resides in the handling of the sensitivities of the global stress constraints. The derivative of Eqn. (11), called c, with respect to a generic density unknown, called ρ_k, may be straightforwardly written as:

$$\frac{\partial c}{\partial \rho_k} = \left[\frac{1}{N} \sum_{i=1}^{N} \left(\frac{\sigma_{VM,i}}{\rho_i^q \sigma_Y} \right)^p \right]^{1/p-1} \cdot \frac{1}{N} \sum_{i=1}^{N} \left[\left(\frac{\sigma_{VM,i}}{\rho_i^q \sigma_Y} \right)^{p-1} \cdot \frac{1}{\sigma_Y} \left(\frac{\partial \sigma_{VM,i}}{\partial \rho_k} \rho_i^{-q} - \delta_{ik} \; q \; \sigma_{VM,i} \rho_i^{-q-1} \right) \right], \quad (13)$$

where δ_{ik} is the Kronecher delta, i.e. $\delta_{ik} = 1$ for $i = k$, otherwise $\delta_{ik} = 0$. One has to take into account that the derivatives of the element–wise stress $\sigma_{VM,i}$ with respect to the density unknowns may be directly solved via a simple analytical computation. It descends from the adoption of the criterion in Eqn. (8) and the independent stress interpolation within the truly–mixed variational principle. One may finally derive the sensitivities of the relevant average degrees of freedom, of the type Eqn. (7), from a set of auxiliary mixed problems:

$$\begin{bmatrix} A_{\sigma\sigma}(\rho) & B_{\sigma u} \\ B_{u\sigma} & 0 \end{bmatrix} \begin{Bmatrix} \dfrac{\partial \sigma}{\partial \rho_k} \\ \\ \dfrac{\partial u}{\partial \rho_k} \end{Bmatrix} = - \begin{bmatrix} \dfrac{\partial A_{\sigma\sigma}}{\partial \rho_k} & 0 \\ \\ 0 & 0 \end{bmatrix} \begin{Bmatrix} \sigma \\ u \end{Bmatrix}. \quad (14)$$

Reference is made to [5] for more details on the adoption of local stress constraints within the mixed framework.

6. Numerical results

To assess the capabilities of the method introduced in the previous sections, a few numerical studies are reported. A rectangular clamped lamina and a L–shaped cantilever are herein investigated to test the alternative p–mean relaxation introduced in Section 5.1 and the numerical procedure detailed in Sections 5.2 and 5.3.

The presented examples may be regarded as preliminary numerical investigations, having the aim of pointing out the main features of the method. Referring to the governing parameters in Eqn. (11), the choice of a high value of p allows in principle to achieve a more homogenous distribution of the stress peaks all over the domain, but has the main counterpart of eventual numerical instabilities that may affect the minimization problem. According to the discussion in [10], the following numerical simulations have been performed adopting $p = 4$.

With regards to SIMP and to the relaxation of the global stress constraint, $q = 2.5$ with $\eta = 3$ is assumed in the sequel.

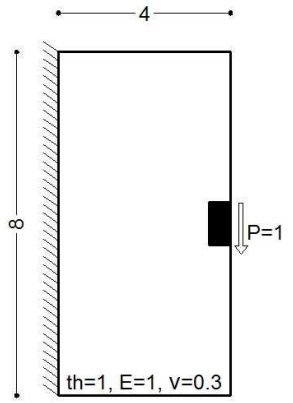

Figure 4: Example 1. A rectangular lamina.

6.1. Rectangular lamina.

The first example deals with the rectangular lamina depicted in Figure 4. The problem is a minimum–weight optimization benchmark, that has been often used in literature to discuss the arising of the singularity problem due to the non–qualifications of stress constraints. The target of the numerical procedure is to distribute the element densities in the white region of the domain according to prescribed average stress values. The black area in Figure 4 refers to zone of full density that are a priori assigned in order to avoid the stress peaks in the vicinity of the load application point. The same cantilever has been tackled in [4] to test, on local stress constraints, the alternative relaxation herein used within the p–mean global enforcement. Figure 5 shows the results of three optimization procedures that have been performed with different values of the allowed strength of material, i.e. $\sigma_Y = 0.60$, $\sigma_Y = 0.50$ and $\sigma_Y = 0.40$, respectively. In all the cases the method achieves final layouts that have a pure 0–1 design and are free from undesired extended gray regions. This means that the proposed global constraint is able to circumvent the singularity phenomenon, thus providing feasible solutions to the considered problem. Figure 6 presents Von Mises stress maps for the final layouts with $\sigma_Y = 0.50$ and $\sigma_Y = 0.40$, respectively. It must be remarked that the values σ_{VM} depicted in the figures are derived from a computation on the three average degrees of freedom of each element, as defined in Eqn. (7) and according to the stress criterion of Eqn. (8). As one may easily see, the mean–nature of the adopted global constraint is not able to avoid the arising of limited regions where the peak stress overcome the allowed σ_Y. However, in agreement with the mechanical behavior of the two–bars problem, the average stress is quite homogeneous all over the domain and seems well–suited to be tackled in manufacturing. Reference is still made to [10] for a discussion on the effect of the choice of σ_Y with respect to the achieved stress peaks within both p–mean and p–norm constraints.

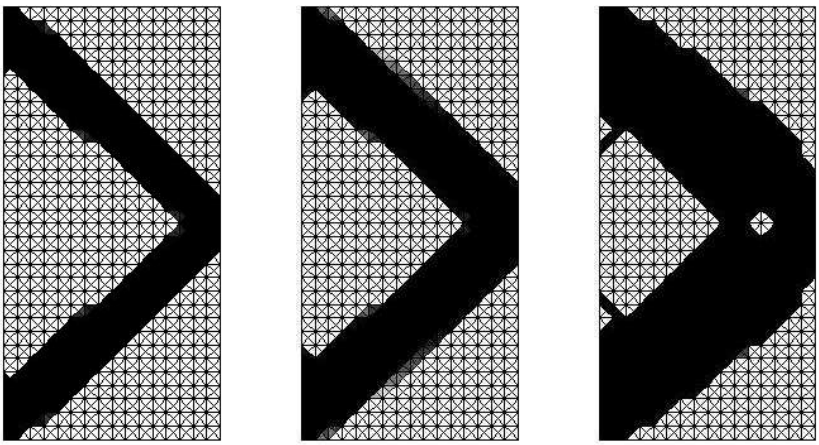

Figure 5: Example 1. Optimal topologies for: $\sigma_Y = 0.60$ (L), $\sigma_Y = 0.50$ (C), $\sigma_Y = 0.40$ (R).

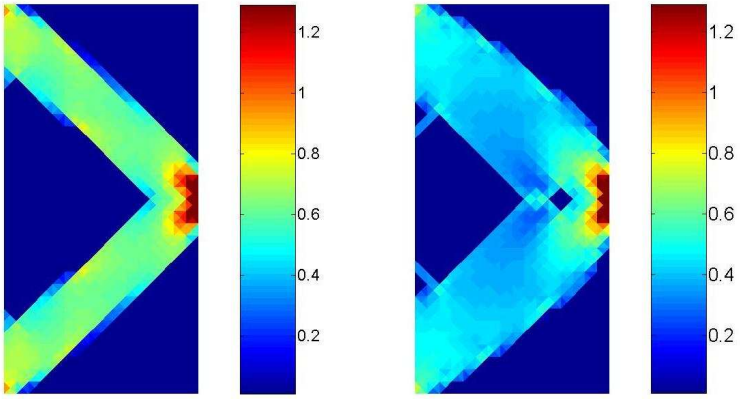

Figure 6: Example 1. Element–wise σ_{VM} for the optimal topologies in Figure 5(C) and (R).

The achieved results strictly respect the imposed p–mean criterion and are in full agreement with the optimal layouts presented in [4], where a relevant number of element–wise local constraints was originally used to drive the minimum weight procedure, at a much higher computational cost. It must be remarked that the truly–mixed method is expected to play a relevant role in the achievement of the optimal designs. Within the framework of an optimization where a single stress constraint governs the overall material distribution, the adoption of such a method allows for a higher accuracy and faster convergence, if compared to low order displacement–based finite element schemes.

6.2. L–shaped cantilever

The second example investigates the benchmark problem in Figure 7, where a remarkable stress concentration arises in the corner zone. Figure 8 shows the optimal topologies achieved for different values of the allowed strength of material, i.e. $\sigma_Y = 0.18$, $\sigma_Y = 0.14$ and $\sigma_Y = 0.12$. As in the previous example final layouts are free from any checkerboarded region or any zone with intermediate material and the achieved results may be regarded as feasible 0–1 structures. The topologies clearly show a remarkable evolution in the material distribution for different requests on the allowed strength. Optimal designs move from the thin struts and ties of Figure 8(L) to the thick arch–like members in Figure 8(R), where the absence of any filtering technique allows for the arising of minor braces that locally bring down the stress. The singularity region of the corner zone makes more difficult to govern both the overall average stress and the local concentration, by means of one single constraint. Figure 9 clearly shows that the considered approach achieves designs where a general homogeneity in the σ_{VM} is perturbed in a few regions by some stress concentrations. However, one has to take into account that the results of Figure 8 may be obtained with a much lower computational cost, with respect to a classical local–constrained solution.

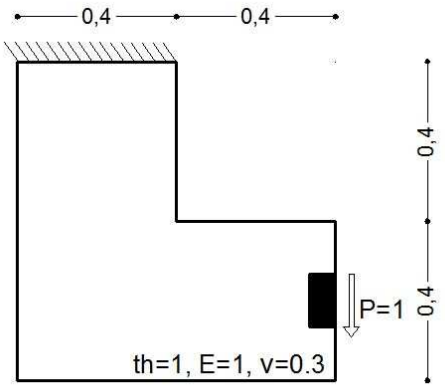

Figure 7: Example 2. A L–shaped cantilever.

The coupling of a limited set of local constraints within the framework of a global p–mean setting may be perhaps considered as an intermediate approach both in terms of computational effort and quality of designs.

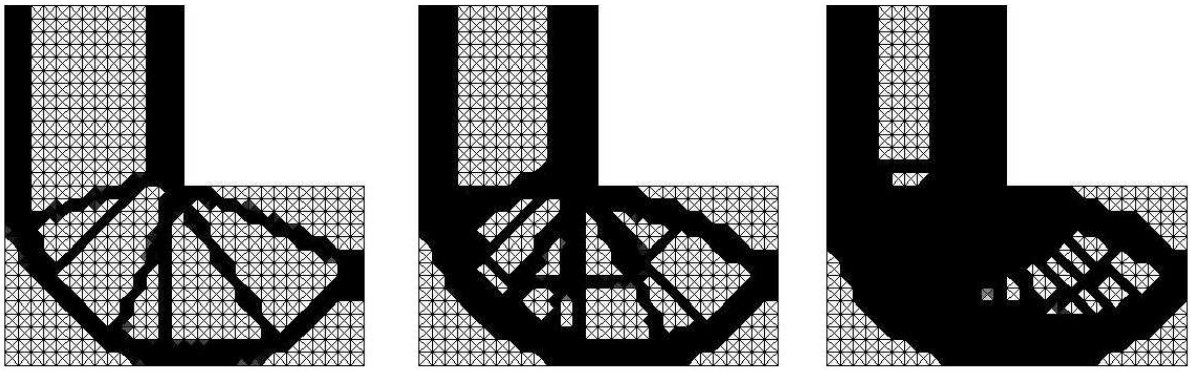

Figure 8: Example 2. Optimal topologies for: $\sigma_Y = 0.18$ (L), $\sigma_Y = 0.14$ (C), $\sigma_Y = 0.12$ (R).

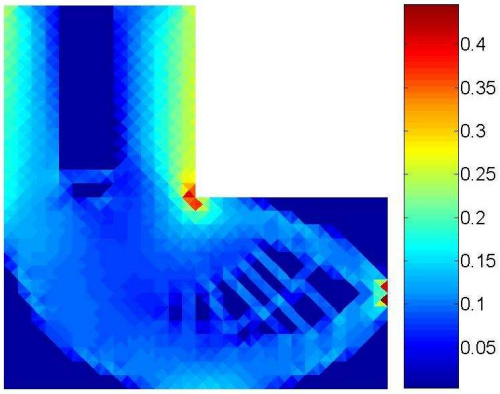

Figure 9: Example 2. Element–wise σ_{VM} for the optimal topology in Figure 8 (R).

7. Conclusions

The contribution has dealt with the implementation of an alternative version of global stress constraint within a minimum–weight optimization, based on truly–mixed finite elements. The adopted global stress measure is a classical p–mean norm where an alternative relaxation has been introduced to tackle the well–known singularity problem. To increase the accuracy in the evaluation of the stress field a robust truly–mixed discretization, based on the composite element of Johnson and Mercier, has been used. A peculiar feature of this finite element scheme allows for an independent interpolation of average degrees of freedom that may be usefully exploited to speed up the computation while preserving a high accuracy in the evaluation of the stress field. The adoption of such a finite element scheme also allows for full stability with respect to incompressible materials. A few preliminary numerical investigations have been performed and discussed, having the main aim of assessing that the proposed methodology is able to find feasible 0–1 designs. Current developments include a wider numerical test on the presented formulation, taking also into account the adoption of a limited set of local constraints to be coupled with the global one. This is expected to improve the achieved designs in the case of the arising of remarkable stress peaks.

8. Acknowledgments

The work is supported by "The 9^{th} Executive Programme for Scientific Cooperation between the Francophone Belgian Community and Italy", years 2009–2010, that is gratefully acknowledged. The first author wishes also to thank Professor Mathias Stolpe for an inspiring discussion on the coupling of truly–mixed methods and stress constraints.

9. References

[**1**] M.P. Bendsoe and O. Sigmund, *Topology Optimization: Theory, Methods and Applications*, Springer–Verlag, Berlin, 2003.

[**2**] D. Braess, *Finite Elements*, Cambridge University Press, 1997.

[**3**] F. Brezzi and M. Fortin, *Mixed and Hybrid Finite Element Methods*, Springer–Verlag, New York, 1991.

[**4**] M. Bruggi, On an alternative approach to stress constraints relaxation in topology optimization, *Structural and Multidisciplinary Optimization*, 36(2), 125–141, 2008.

[**5**] M. Bruggi and P. Venini, A mixed FEM approach to stress–constrained topology optimization, *International Journal for Numerical Methods in Engineering*, 73, 1693-1714, 2008.

[**6**] G.D. Cheng and X. Guo ε–relaxed approach in topology optimization, *Structural Optimization*, 13, 258–266, 1997.

[**7**] G. Cheng and Z. Jiang Study on topology optimization with stress constraints, *Engineering Optimization*, 20, 129–148, 1992.

[**8**] G. Duvaut, *Mécanique de Milieux Continus*, Masson, 1992.

[**9**] P. Duysinx and M. Bendsøe, Topology optimization of continuum structures with local stress constraints, *International Journal for Numerical Methods in Engineering*, 43, 1453–1478, 1998.

[**10**] P. Duysinx and O. Sigmund, New developments in handling stress constraints in optimal material distribution. *Seventh Symposium on Multidisciplinary Analysis and Optimization*, AIAA-98-4906, 1501-1509, 1998.

[**11**] C. Johnson. and B. Mercier, Some equilibrium finite elements methods for two dimensional elasticity problems, *Numer. Math.*, 30, 103–116, 1978.

[**12**] O. Schenk and K. Gärtner, Solving Unsymmetric Sparse Systems of Linear Equations with PARDISO, *Journal of Future Generation Computer Systems*, 20(3), 475–487, 2004.

[**13**] O. Schenk and K. Gärtner, On fast factorization pivoting methods for symmetric indefinite systems, *Elec. Trans. Numer. Anal.*, 23, 158–179, 2006.

[**14**] O. Sigmund and P.M. Clausen, Topology optimization using a mixed formulation: An alternative way to solve pressure load problems *Comput. Methods Appl. Mech. Eng.*, 196, 1874–1889, 2007.

[**15**] K. Svamberg, Method of moving asymptotes - A new method for structural optimization. *International Journal for Numerical Methods in Engineering*, 24(3), 359–373, 1987.

[**16**] S.P. Timoshenko and J.N. Goodier, *Theory of Elasticity*, McGraw-Hill, New York, 1970.